Molecular clouds in the Perseus arm

Wouterloot, J.G.A.; Habing, H.J.

Astron. Astrophys. 151, 297–308 (1985)

ASTRONOMY AND ASTROPHYSICS

Molecular clouds in the Perseus arm

J.G.A. Wouterloot* and H.J. Habing

Sterrewacht, Postbus 9513, NL-2300 RA Leiden, The Netherlands

Received May 19, 1983; accepted April 17, 1985

Summary. We report on 18 cm OH observations of molecular clouds in a section of the Perseus spiral arm. First we searched approximately 160 square degrees with the 25 m Dwingeloo telescope and detected five Perseus arm clouds. These were studied in more detail with the 100 m Effelsberg telescope. Secondly we made OH observations in the direction of a number of clouds, detected during a CO survey of the Perseus arm by Cong (but not found in Dwingeloo). We detected OH in 24 clouds, including the 5 mapped clouds. The data suggest a relation between cloud mass and radial velocity, the most massive clouds having a more negative velocity. This is explained by an existing density wave model for this part of the Perseus arm. The properties and distribution of the clouds are compared with those of other spiral arm tracers.

Key words: OH emission – molecular clouds – Perseus arm

1. Introduction

The Perseus arm is suitably located to study its structure directly and in some detail and many such studies have been made. Its distance is reasonably small and a large part is viewed under a very favourable angle. No other (major) arms are seen projected behind the Perseus arm: most objects in it can be recognized individually.

The Perseus arm also has some disadvantages: the rotational velocity outside the solar circle is not very well known and kinematical distances are uncertain (in particular due to possible streaming motions). The arm is located at a large distance from the galactic center where the shock, expected from the density wave theory is much weaker than in the inner arms. This will probably decrease the star or cloud formation rate and may therefore have profound effects on the arm as a whole; in other words: the arm may be poorer in spiral arm tracers than arms further inward. To obtain insight into the properties of molecular clouds in a spiral arm and their relation to other spiral arm tracers, we observed a sample of clouds situated in the Perseus arm in OH at 1665 and 1667 MHz. The observational methods are described in section 2. The results of the OH observations are presented and analysed as far as the individual clouds are concerned in Sect 3. In Sect 4 the properties of the OH clouds in relation with other spiral arm tracers are discussed and a general picture of the structure of the Perseus arm is given.

Although Perseus arm objects have different distances to the sun at different longitudes, in deriving cloud parameters we shall assume that all objects belonging to the Perseus arm are at 3.5 kpc distance.

2. The observations

The Dwingeloo observations (beam size 31′, beam efficiency 0.76) were made on a grid with spacings of 0°.3 in galactic longitude and latitude. In longitude the area extends from $l = 100°$ to 139°. The latitude extent is irregular, on average from $-1°.7$ to $+2°.5$, and was chosen to include as many optically known HII regions in the Perseus arm as possible. The observations were made at 1667 MHz with a resolution of 0.9 km s^{-1} and an integration time of 30 minutes. This resulted in an r.m.s. noise level of about 0.02 K. We observed in total power mode with a reference measurement at the North Pole every 12 hours.

We found many clouds of large angular extent and a small radial velocity, that are clearly local objects (see Wouterloot, 1981-chapter 6). Also we detected five clouds with a radial velocity between -40 and -60 km s^{-1} which means that they belong to the Perseus arm. These clouds were mapped in OH with the Effelsberg telescope (beam size 7′.8, beam efficiency 0.70) on a grid with spacings of 7′.5. We used a resolution of 1.1 km s^{-1} and an integration time of 30 minutes, while switching the frequency with the signal appearing in both bands. The two main lines (at 1665 and 1667 MHz), were observed simultaneously. A second set of observations at Effelsberg concerned clouds in the Perseus arm discovered by Cong in the CO ($J = 1 - 0$) transition with the Columbia telescope and made available to us by him. The center positions of these clouds were observed with the same resolution and integration time as the other clouds. At some positions we made additional observations with better velocity resolution to see whether the line consisted of more than one component. Finally, we made an observation with a resolution of 0.07 km s^{-1} of the NGC 7538 1720 MHz maser. Left and right circular polarization were observed simultaneously.

During part of the observations at Effelsberg the two channels of the receiver system were saturated unequally. Corrections to

Send offprint requests to: J.G.A. Wouterloot

* Present address: Max-Planck-Institut für Radioastronomie Auf dem Hügel 69, D-5300 Bonn 1, Federal Republic of Germany

the intensities could amount to a factor of two and remaining uncertainties of the relative intensities of the two lines are about five percent.

3. Observational results

3.1. Mapping results

We define $T_{A,i}$ to be the peak antenna temperature of a spectral feature, where i refers to the specific transition ($i = 1, 2, 3, 4$: 1612, 1665, 1667, 1720 MHz). All 1667 MHz spectra were inspected visually. A peak with $T_{A,3} \geq 0.08$ K (4σ) was considered real, if it occurred at two adjacent positions. Five such cases were detected. Weaker features or signals appearing at only one position were remeasured for confirmation, always without success. Since we covered the search-area with a grid of positions separated by about 0.6 beamwidths, we expect to have detected all clouds with $T_B > 0.2$ K and larger than 25 pc. Of course, smaller clouds or fainter ones probably have been missed. The observed part of the Perseus arm (163 square degrees or 0.6 kpc^2 at 3.5 kpc distance) thus appears to contain 5 large clouds. They are listed in Table 1; column 4 therein lists the number of positions with $T_{A,3} > 0.06$ K to indicate the angular area of the cloud. Column 5 gives the highest value at $T_{A,3}$. After detection the five clouds were mapped with the 100 m telescope.

Table 1. Clouds detected in Dwingeloo

l	b	V	N	$T_{A,3}$	Rel. obj.
104.8	0.3	−55.0	3	0.09	–
108.7	0.3	−54.2	4	0.10	–
110.0	−0.3	−51.2	5	0.13	S156
111.5	0.6	−53.6	7	0.10	S158
132.8	0.9	−43.0	3	0.12	W3

3.1.1. Cloud 104.8 + 0.3

The peak antenna temperature for the 100 m telescope is 0.11 K, and it was detected only at a few positions. A rough contour map is shown in Fig. 1. This cloud is very isolated and apparently not associated with an HII region. The diameter is 22 pc. The line ratio $T_{A,3}/T_{A,2}$ could not be measured with sufficient accuracy. If for the 1667 MHz line we adopt optical depth $\tau_3 = 0$, excitation temperature $T_{ex,3} = 5.5$ K, and an OH/H_{tot} abundance of $6\,10^{-8}$ (these values are representative for local clouds; Wouterloot, 1981), the mass is $6.9\,10^3\,M_0$. The cloud is outside the longitude range observed in the CO survey by Cong, and no additional information is available.

3.1.2. Cloud 108.3 + 0.3

A contour map is shown in Fig. 2. There are two regions with a peak antenna temperature of about 0.2 K. One of those peaks corresponds with the position of maximum emission in CO (Cong, private communication). The extent of this cloud is about 30 pc. The velocity is constant at -52.8 km s^{-1} and the linewidth is

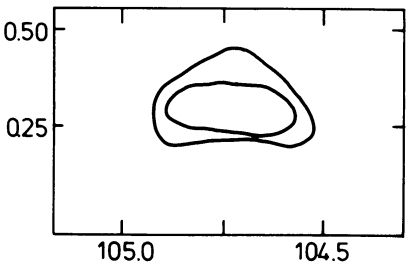

Fig. 1. 1667 MHz map of cloud 104.8 + 0.3. Contour values are 0.07 and 0.10 K

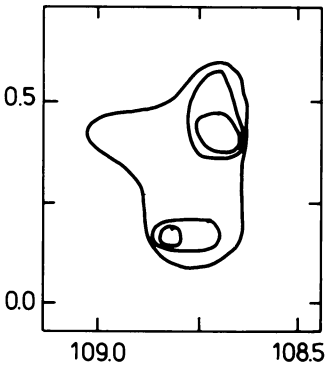

Fig. 2. 1667 MHz map of cloud 108.7 + 0.3. Contour values are 0.10, 0.15 and 0.20 K

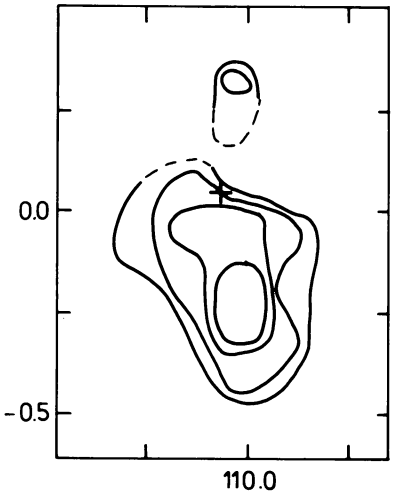

Fig. 3. 1667 MHz map of cloud 110.0 − 0.3. Contour values are 0.07, 0.10, 0.15 and 0.20 K. S156 is indicated by a plus sign.

2.3 ± 0.9 km s^{-1} for both transitions. The line ratios point to a low value for τ_3. For $\tau_3 = 0$ the mass is $1.6\,10^4\,M_0$. We have not found an association of this cloud with other objects.

3.1.3. Cloud 110.0 − 0.3

This cloud is connected with the HII region S156 (see e.g. Heydari-Malayeri et al., 1980). Höglund and Gordon (1973) first discovered this cloud in OH and H_2CO. Figure 3 shows the Effelsberg OH map at 1667 MHz. A cross indicates the position of S156.

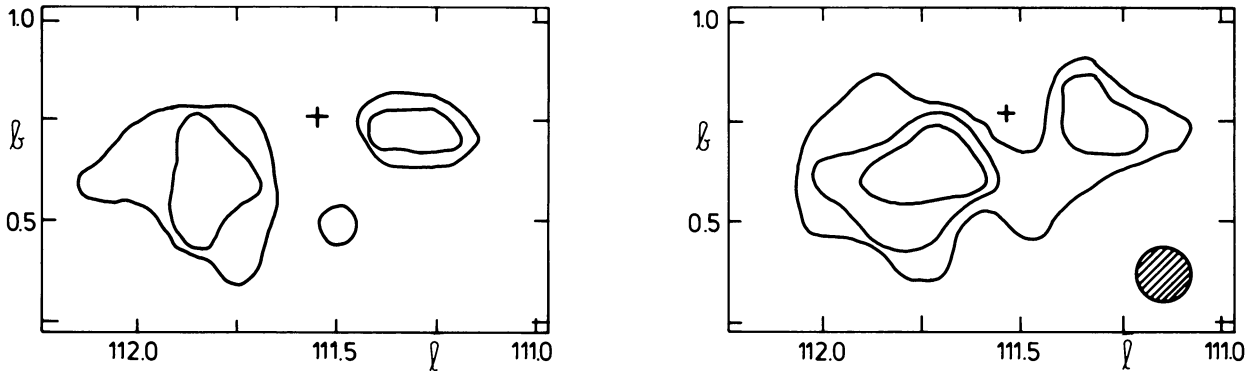

Fig. 4. 1665 (left) and 1667 MHz (right) map of cloud 111.5 + 0.6. Contour values are 0.07, 0.10 and 0.15 K. The position of the maser source is indicated by a plus sign.

Higher resolution H_2CO observation by Winnberg (private communication) revealed that the ~ 0.2 K core of the cloud consists of three fragments, each of about 5 pc, embedded in more extended emission. The length of the OH cloud is 36 pc with a probable extension to 50 pc, although the lines are rather weak in the high latitude part of the cloud. Winnberg also found that the cloud extends to positive latitudes above S156. At the lowest latitudes the velocity is systematically somewhat larger (~ 0.5 km s^{-1}), suggesting the presence of a small velocity gradient. Assuming a distance of 3.5 kpc and $\tau_3 = 0$, the mass is $4.4\,10^4\,M_0$. Using the equations of Cohen et al. (1983) we obtain, from the H_2CO observations, a mass of $2.4\,10^4\,M_0$.

3.1.4. Cloud 111.5 + 0.6

This cloud is near the HII region NGC 7538 (or S158). We refer to Read (1980) for a summary of previous studies. The molecular cloud associated with S158 was discovered in H_2CO by Minn and Greenberg (1975). They detected three clouds, which they called complexes 1 to 3, with different radial velocities, all at least 5 km s^{-1} larger than that of the HII region. The OH maps at 1667 and 1665 MHz are shown in Fig. 4. The plus sign indicates the position of the NGC 7538 OH-maser. The absence of OH emission there is misleading: due to strong maser emission we could not recognize the weak emission from any cloud material. The higher longitude part (complex 3) is larger than the part at the other side of the maser (complex 1). The mean OH velocities, -52.4 and -54.4 km s^{-1} agree with those of the H_2CO. Complex 2 was not detected in OH. A clear jump in radial velocity indicates that the radial velocity of cloud 111.5 + 0.6 does not vary continuously, but that the two complexes (1 and 3) are separate, a situation similar to that of the Mon OB1 area (Wouterloot, 1984). The clouds are more extended in OH than in H_2CO. This is probably not due to the 40% larger OH beam but reflects the difference in OH and H_2CO abundance. Minn and Greenberg (1975) found very broad (about 5 km s^{-1}) H_2CO lines. The mean value of the OH linewidth for both complexes is 3 ± 0.5 km s^{-1}, somewhat larger than in the other Perseus arm clouds. In contrast to Minn and Greenberg we do not find indications for a larger linewidth in the cloud center. We assume that in both complexes $\tau_3 = 0$; there is some indication that in complex 1 the optical depth is significant, but the accuracy of this result is too low to derive a reliable value for τ_3. For zero optical depth the masses are respectively $1.3\,10^4\,M_0$ (complex 1) and $3.9\,10^4\,M_0$ (complex 3). Because of optical depth effects the mass of complex 1 may have been underestimated.

Figure 5 shows the left and right circularly polarized spectra, made on May 29 1979 with high resolution (0.07 km s^{-1}) of the 1720 MHz maser source near NGC 7538 observed at the position given by Wynn-Williams et al. (1974). These authors and Hardebeck (1971) previously observed the source with lower velocity resolution (0.7 km s^{-1}). The components that we detected are listed in Table 2. The line at -59.3 km s^{-1} has linewidths of 0.21 and 0.27 km s^{-1} for the two polarizations with a possible,

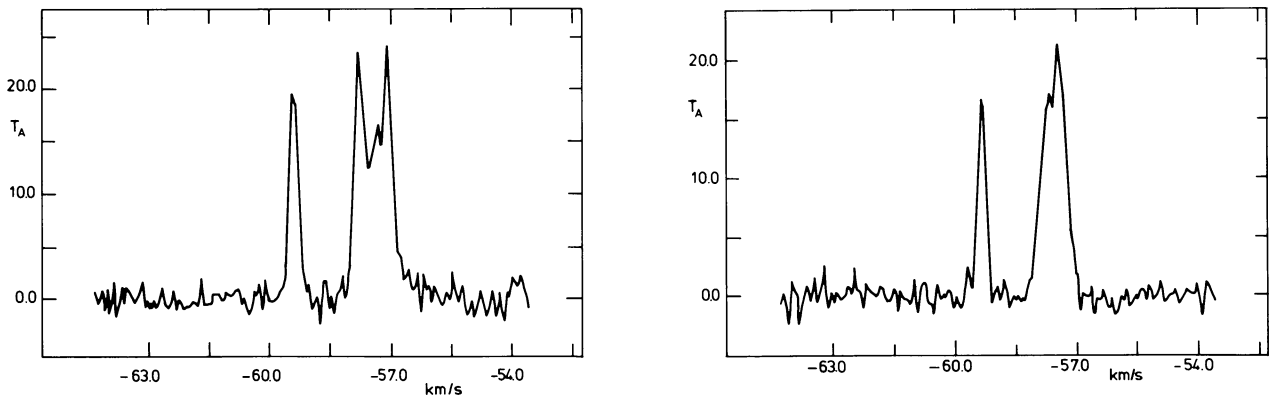

Fig. 5. Left (left) and right (right) circularly polarized spectra at 1720 MHz of the maser source near NOC 7538.

Table 2. Line parameters of NGC 7538 1720 MHz maser

Pol	V km s^{-1}	T_A K	F Jy	LW km s^{-1}
L	−59.39	19.4	6.8	0.27
	−57.77	23.6	8.3	0.35
	−57.35	16.9	5.9	0.03
	−57.12	24.0	8.4	0.30
R	−59.31	17.2	6.0	0.21
	−57.66	17.1	6.0	0.30
	−57.43	21.6	7.6	0.30

but not yet significant, velocity difference of 0.08 km s^{-1} between left and right circular polarization (LC resp. RC). The other line has a more complex structure and is at least partly circularly polarized. Guilloteau and Lucas (1981) observed this source in April 1981 with 0.03 km s^{-1} resolution. The −59.3 km s^{-1} components have changed little between the two observations and the difference in velocity seems to be real. However the −57 km s^{-1} components show strong variability in both polarisations and a new component appeared at −56.6 km s^{-1}.

3.1.5. Cloud 132.8 + 0.9

This cloud is a part of the W3 complex. Coudis (1979) reviewed the observations in this area. OH was first detected by Höglund and Andersson (1978). They found an antenna temperature of 0.055 K with a 29′ beam. The cloud was mapped previously in CO by Lada et al. (1978). In our observations we noticed strong radiation from the maser source W3(OH) through the sidelobes of the telescope beam up to distances of 30 arcmin. The strong maser emission makes it impossible to find any cloud emission near the position of W3 and of W3(OH). Maps of the 1665 and 1667 MHz peak antenna temperatures are shown in Fig. 6. The two maxima at 1667 MHz coincide with peaks in the high resolution (2′.3) CO map by Lada et al. Two peaks at lower latitude in the low resolution CO map were not detected in OH. In this region Hasegawa et al. (1980) found signs of HI self absorption. The absence of OH in regions with HI self absorption is uncommon as other such regions show, e.g. Cloud 2 or the ρ Oph cloud (Wouterloot, 1981). Possibly the interpretation of self absorption in this case is incorrect: molecular emission in the region is seen at various velocities between −40 and −50 km s^{-1}. If all clouds are associated with an HI cloud, the total line profile might be sufficiently bumpy by itself, without any self absorption. We have made high velocity resolution (0.3 km s^{-1}) observations at the two positions of maximum $T_{A,3}$: at (132°.975, 0°.775) and at (133°.225, 0°.9). The spectra are shown in Fig. 7. The lines are well resolved with a total width of 20 km s^{-1} at 1667 MHz at both positions. The antenna temperature at the first position (Fig. 7, left), 0.62 K, is very high in view of the low resolution, 5.9 pc, and the area deserves some more detailed observations. The line ratio at this position is about 2.0 (low OH opacity), at the other it is about 1.0 (large OH opacity). Because the spectra were taken in succession the difference in optical depth is probably real. In the rest of the cloud the line ratio is systematically higher near position 1 than near position 2, although an accurate value cannot be determined due to the calibration problems mentioned in Sect. 2. There may be a velocity gradient in the complex, in particular near position 2 where the radial velocity decreases with latitude from about −42 to −44 km s^{-1}. We derive the mass in two ways. First we take $\tau_3 = 0$ everywhere in the cloud. Then we take $\tau_3 = 0$ near position 1 and $\tau_3 = 2$ near position 2. The total mass of the cloud is then respectively 4.4 10^4 $M_\odot$ and 5.6 10^4 $M_\odot$. This is in agreement with the result by Lada et al. ($\leq 3.0 \times 10^4$ $M_\odot$) if one takes into account that they adopted a distance of 2 kpc.

3.2. Clouds discovered first in CO

With the 1.2 m telescope at Columbia University, New York, Cong observed the Perseus arm in ^{12}CO between l = 105° and l = 140°. Cohen et al. (1980) presented some results of this survey. From a preliminary list, put at our disposal, we selected the CO clouds with the highest temperatures and searched for OH with the Effelsberg telescope at the CO peak position. Of the 61 CO

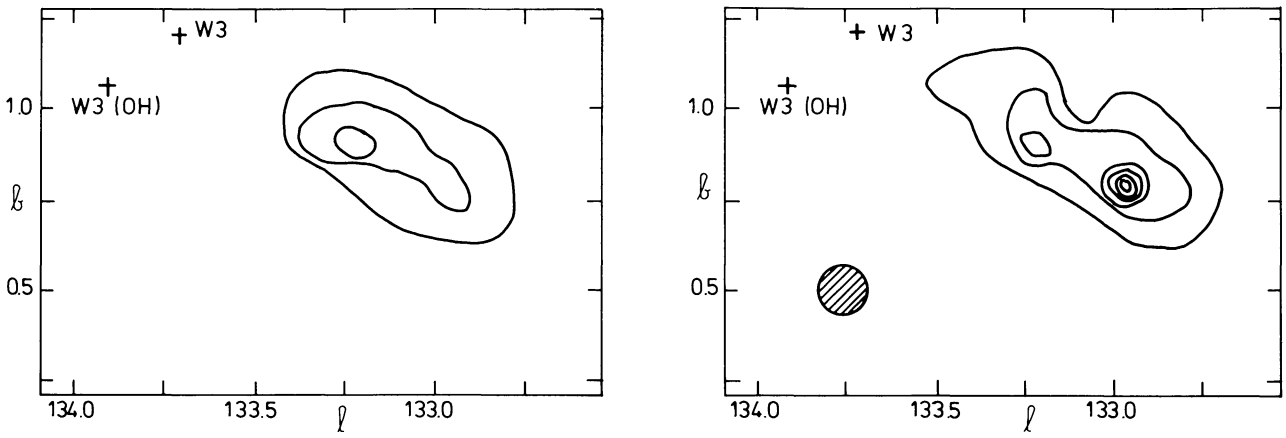

Fig. 6. 1665 (left) and 1667 MHz (right) map of cloud 132.8 + 0.9. Contour values are 0.10, 0.20, 0.30, ... K

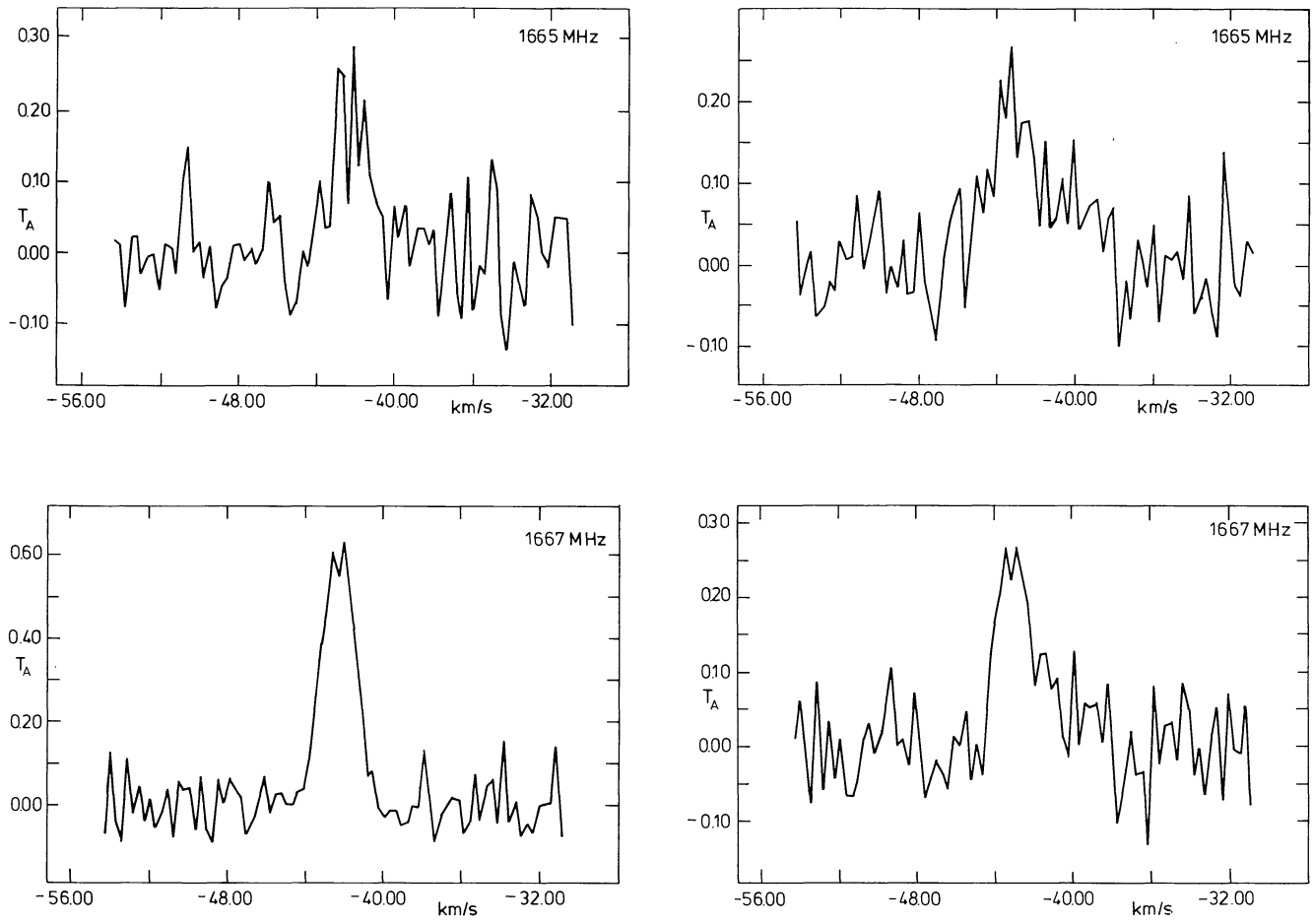

Fig. 7. High resolution 1665 and 1667 MHz spectra at (132.975, 0.775), left and (133.225, 0.9), right

positions in Cong's list we observed 29 and detected OH at 22 positions in at least one line. The results are shown in Table 3. At some positions the line profile contained more than one component, e.g. position 22 also shows the emission of a local cloud. Three clouds (nrs. 27, 28 and 30) were detected in absorption against continuum sources, near W4 and W5. A very narrow absorption line is seen in front of S201. All line ratios indicate thermal emission except at one position near the HII region S152 (see below).

CO data and other information are listed in Table 4. Column 2 contains the CO antenna temperature and column 3 the corresponding excitation temperature (Cong, private communication). Column 4 shows an effective CO linewidth, obtained by dividing the integrated line intensity by the peak antenna temperature. In column 6 is the possibly related HII region with its radial velocity in column 7 (Humphreys, 1976, Crampton et al., 1978). Column 8 gives a mean diameter, measured between points where the CO antenna temperature is about half its peak value. Column 9 shows the velocity of maximum HI emission at each position, obtained from the Maryland-Greenbank survey (Westerhout and Wendlandt, 1982) as follows. For each cloud we made an HI latitude-velocity diagram at the longitude of the cloud center. In general the HI has its maximum intensity at a single velocity around $-50\,\mathrm{km\,s^{-1}}$. In only a few cases the HI line showed two or more components, apparently not caused by self absorption; then we used the one closest in velocity to the molecular cloud. HI self absorption was found at four positions. The column-density N_{OH} has been calculated by assuming $\tau_3 = 0$, because the signal to noise ratio of the 1665 MHz line was too small to derive τ_3 directly. This means that our value of N_{OH} is a lower limit. For the five clouds discussed before, the value of N_{OH} in Table 4 is an average for all positions where both lines were detected. To estimate the column densities at positions where OH is in absorption, we used the continuum observations of Wendker and Altenhoff (1977) at 11 cm and of Rohlfs et al. (1977) at 21 cm.

At position 3 (near S152) we detected not only thermal 1667 MHz emission (at the CO velocity of $-51\,\mathrm{km\,s^{-1}}$), but also very narrow 1665 MHz emission at a different velocity. We subsequently observed this feature with a higher resolution (0.15 km $\mathrm{s^{-1}}$) and obtained a more accurate position: $\alpha(1950) = 22^h\,56^m\,40^s$, $\delta(1950) = 58°29'51''$. The uncertainty is large (about 45″ in α and δ) due to the weakness of the lines. This maser source has three components, all 100% circularly polarized. One LC component of 0.64 Jy is at $-43.46\,\mathrm{km\,s^{-1}}$ with a total line width of $0.45\,\mathrm{km\,s^{-1}}$, including a weaker line of about 0.3 Jy at $-42.96\,\mathrm{km\,s^{-1}}$. An RC component of 0.16 Jy is at $-48.80\,\mathrm{km\,s^{-1}}$ and has a linewidth of $0.2\,\mathrm{km\,s^{-1}}$. The positional accuracy excludes its coincidence with the compact HII region, observed by Israel (1977), but it is very nearby (57″). The radial velocity is about $-44\,\mathrm{km\,s^{-1}}$ (Crampton et al., 1978) close to that of the maser source.

Table 3. Observed parameters

Nr	l	b	$T_{A,3}$	ΔV	V	$T_{A,2}$	ΔV	V
1	104.7	0.3	0.11	2.1	−53.7	0.06	2.3	−53.8
2	10.5.625	0.375	<0.06			<0.07		
3	108.75	−1.0	0.11	2.1	−51.0	<0.07	2.4	−52.7
4	108.7	0.25	0.15	2.2	−52.9	0.07	2.4	−46.7
5	109.0	−0.25	0.11	3.4	−47.6	0.09	2.7	−46.7
6	109.875	−1.25	<0.06			<0.06		
7	110.125	0.0	0.19	2.8	−52.0	0.08	3.1	−52.2
8	111.25	−3.125	0.10	4.0	−43.2	0.04	3.0	−43.2
9	111.25	−1.5	<0.08			<0.06		
10	111.25	−6.25	0.10	1.4	−48.8	<0.06		
11	111.5	0.75	0.12	3.3	−53.4	0.09	2.6	−53.4
12	111.5	1.25	0.14	3.2	−46.0	<0.06		
13	111.625	−3.5	0.12	1.3	−42.3	0.10	1.3	−45.2
14	112.125	−2.5	<0.05			<0.08		
15	113.0	−0.75	0.15	1.3	−33.7	<0.06		
16	114.5	−0.5	0.09	2.0	−47.7	0.16	1.5	−48.9
17	115.75	−1.625	<0.05			<0.05		
18	117.0	−2.25	0.09	4.6	−42.9	<0.08		
19	118.625	−1.375	0.07	5.9	−40.0	<0.07		
20	120.125	2.125	0.08	3.4	−50.0	<0.07		
21	120.625	−0.375	0.08	4.7	−46.7	<0.06		
22	123.125	−0.875	0.11	2.0	−57.0	0.11	1.1	−57.9
			0.13	2.4	−44.5	0.09	1.8	−44.9
			0.12	2.0	−18.7	0.08	1.5	−18.4
23	132.88	0.79	0.24	2.6	−42.4	0.15	2.2	−42.7
24	133.28	0.49	0.07	3.5	−48.3	<0.06		
25	133.51	0.1	0.18	2.3	−43.0	–		
26	133.82	0.54	<0.06			–		
27	134.15	0.81	−0.30	3.9	−50.0	−0.26	3.9	−50.0
28	136.88	1.11	−0.18	2.5	−41.5	0.11	2.5	−41.6
29	137.68	1.52	<0.10			<0.05		
30	138.52	1.65	−0.19	1.3	−39.1	−0.09	1.3	−39.1

4. The structure of the perseus arm

4.1. The relation between clouds, HII regions and OB associations

Figure 8 displays the positions of objects located in the Perseus arm between $l = 100°$ and $l = 140°$. Shown are optical HII regions (Georgelin, 1975; Crampton et al., 1978; Humphreys, 1976), molecular clouds (Cong, private communication), young clusters (Georgelin, 1975; Humphreys, 1976) individual members of OB associations (Humphreys, 1978) and supernova remnants (Milne, 1979; Kallas and Reich, 1980; Hughes et al., 1980). The total halfwidth of the distribution in latitude is equal for clouds and HII regions and is about 120 pc.

To study the relation between the molecular clouds and HII regions we used the radio continuum survey by Kallas and Reich (1980), who observed the galactic plane between $l = 90°$ and $l = 162°$ with a sensitivity limit of 0.3 Jy for point sources and a resolution of 9′. Of all the CO clouds in the Perseus arm between $l = 104°$ and $l = 130°$ only 11 (25%) are associated with a radio source, eight of which coincide with an optical HII region. Of the remaining three radio sources one is very weak and possibly not real. Because some of these three may be non-thermal background sources, only very few large HII regions have escaped detection. Of course, many of the clouds may still be associated with weak, but compact HII regions that have not been picked up in the radio continuum survey. However, five clouds are too near to CasA to obtain information on any associated radio continuum source.

The relation between stellar OB associations and molecular clouds is not as straightforward as it is in the direct solar neighbourhood (see e.g. Blitz, 1978). The OB associations in the Perseus arm are often several hundred parsec across (see Fig. 8), whereas those in the solar neighbourhood are much smaller (Blaauw, 1964). In many cases more than one cloud is seen in projection against each association. Then either one of these clouds is connected with the stellar association or they all are, in which case the stellar association probably consists of several subgroups that have not yet been recognized as such. Unambiguous cases are those of the Cas OB6 association, which is connected to the W4 complex, and of Per OB1 which apparently is not related to any molecular cloud. Also Cep OB5 and Cas OB8 show no clouds projected within their boundaries. In all other cases the connec-

Table 4. Other information of clouds observed in OH

Nr	T_{CO} (K)	T_{ex} (K)	ΔV_{eff} (km s^{-1})	V_{CO}	HII	$V_{H\,II}$ (km s^{-1})	V_{HI}	Size (degrees)	N_{OH} (cm^{-2})
1							−51.5	0.3	2.1 10^{14}
2	3.1	6.3	5.4	−52.0	S138	−60.0	−56.1	0.5	1.1
3	5.0	8.3	4.8	−51.1	S152, S153	−44.3	−49.0	0.7	2.1
	1.5	4.6		−47.3					
4			(6.3)				−47.5	0.6	2.9
	3.0	6.2		−52.5					
5	4.5	7.8	4.4	−47.5			−45.5	0.5	3.1
6	2.0	5.1	6.5	−33.0			−43.0	0.3	1.1
7	6.5	9.8	5.9	−51.8	S156	−51.7	−47.0	0.8	4.7
	3.7	6.9		−41.5					
8			(13.8)	—				0.8	3.7
	2.5	5.7		−34.9					
9	2.5	5.7	9.6	−39.4			−43.0	0.5	1.4
	2.4	5.6		−43.1					
10			(6.7)		S157	−46.6	−47.5	0.3	1.2
	1.6	4.7		−47.5					
11	6.5	9.8	12.0	−55.4	S158	−59.5	−48.5	1.0	3.5
12	3.3	6.5	5.5	−46.2			−47.5	0.4	4.0
13	1.9	5.0	13.2	−45.2			—	0.4	1.4
14	2.5	5.7	7.6	−37.5			−39.0	0.5	0.9
15	1.3	4.4	7.7	−34.5			−49, −40.5	0.3	1.7
16	3.5	6.7	4.9	−49.4			−46.5	0.5	1.6
17	4.5	7.8	3.6	−39.2	S168, S169	−44	−39.0	0.4	0.9
18	2.0	5.1	6.0	43.8			−48.5	0.4	3.9
19	2.6	5.8	4.6	−39.1	S172		−40.0	0.3	3.7
20	2.5	5.7	3.6	−50.3	S175	−50.7	−49.0	0.3	2.4
21	1.4	4.5	7.1	−46.3	S177		−45.5	0.3	3.3
22									2.0
	2.9	6.1	5.5	−44.5			−41.0	0.6	2.8
									2.1
23	3.4	6.6	4.7	−42			−44.0	0.4	5.6
24	2.2	5.4	7.7	−50			−54.0	0.4	2.2
25	3.9	7.2	5.4	−43			−52.0	0.4	3.7
26	3.6	6.8	5.6	−47			−51.5	0.4	1.1
27	4.0	7.3	5.5	−50			−52	0.4	9
28	3.9	7.2	8.2	−40			−50	0.3	4
29	4.3	7.6	4.4	−39			−41.0	0.3	1.8
30	3.0	6.2	7.0	−38	S201		−41.5	0.3	3

tion between clouds and OB associations is ambiguous and the issue will not be pursued until more elaborate (optical) data are available.

In Figure 8 we have included also supernova remnants (SNR's) because they may function as triggers of star formation. There are 10 SNR's known in the direction of the part of the Perseus arm discussed here. They are equally distributed in longitude, but four of them (all around $l = 130°$) are outside the boundaries of the associations. However, the SNR ages are probably too small to show any noticeable effect on the clouds.

4.2. Properties of the sample of clouds

We divide the 29 CO clouds observed in OH and listed in Tables 3 and 4 into three groups: group 1, no OH detected; group 2, only detected at 1667 MHz; group 3 detected at both 1665 and 1667 MHz. Figure 9 shows a histogram of the radial velocities of all CO clouds with $l < 130°$; the clouds observed in OH have been indicated by the number of the group to which they belong. The mean velocity of all CO clouds, -49.9 ± 7.3 km s^{-1}, is the same as that of those observed also in OH, -44.4 ± 6.2 km s^{-1}. However, there is a systematic shift in CO velocity from OH clouds in group 1 to those in group 3. This is not a consequence of a different distribution in longitude. The result is shown again in Table 5, which contains various average parameters for each group. The first two lines show no significant variations from group to group. Most significant is the effect seen in the last two lines of Table 5: the average velocity decreases strongly from group 1 to group 3, and $V_H - V_{CO}$ increases. One can question the reality of these effects, because they are based only on those CO clouds which have the highest T_{CO}. The velocity distribution of the clouds not observed in OH is the same, but in principle it

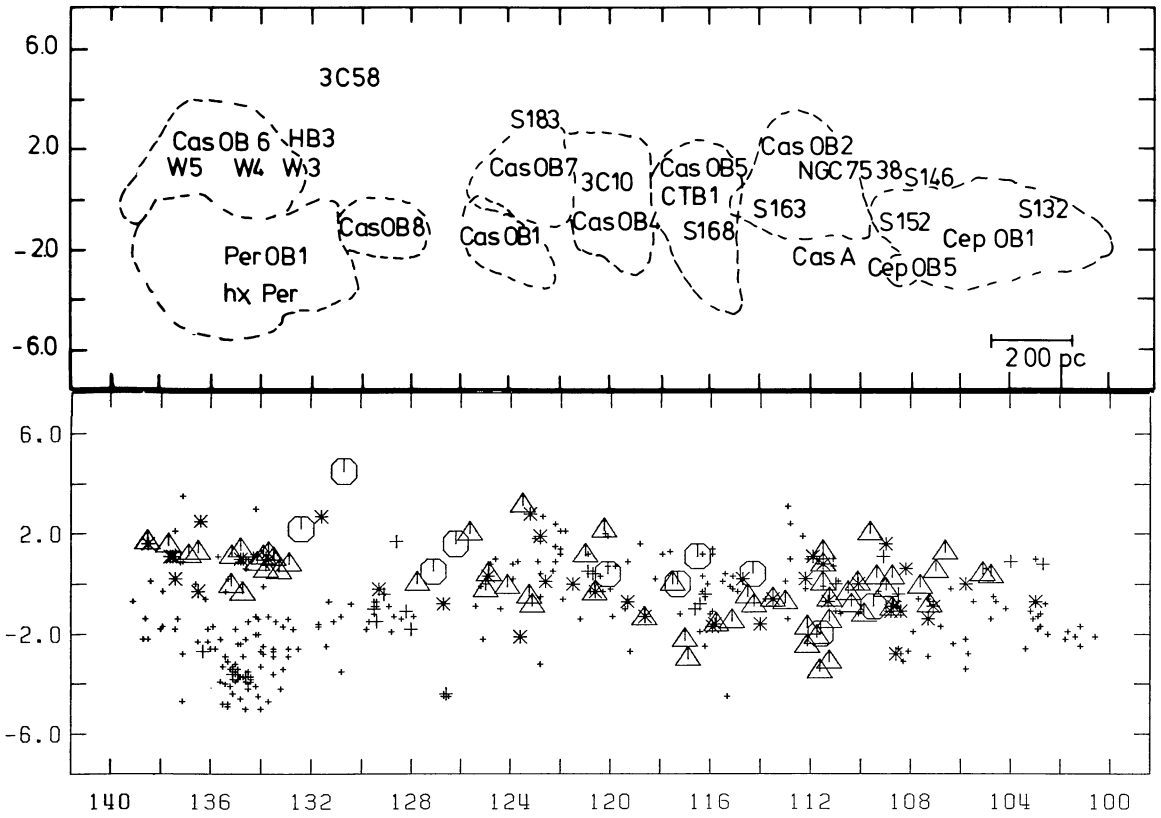

Fig. 8. The distribution of Perseus arm objects. Shown are OB stars (small +) young clusters (large +), HII regions (*), molecular clouds (Δ) and supernova remnants (○). In the upper part of this figure the extent of the associations is indicated, together with the position of some individual objects

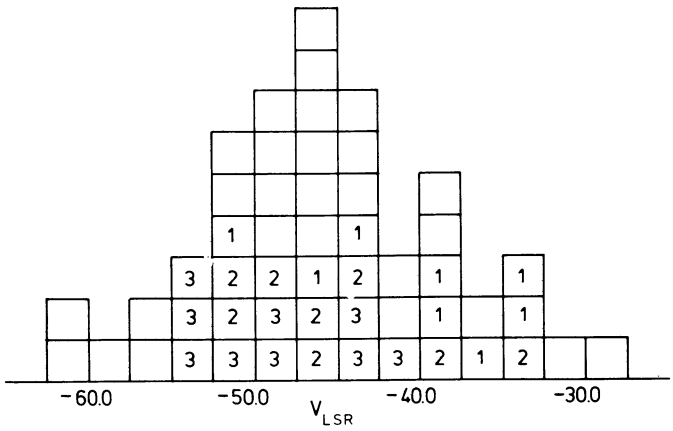

Fig. 9. Histogram of cloud velocities between $l = 100°$ and $l = 130°$ for CO clouds and OH clouds of groups, 1, 2 and 3

is possible that they contribute to the groups 1 to 3 in a different way. We made some t-tests of the significance of our result. Using the sample of observed clouds the probability that the velocity difference between the groups 1 and 3 is real, is 99%. If the non-observed clouds are included in the sample by dividing them equally over the groups 1 and 3 this number changes to 85% and if all non observed clouds are counted in groups the significance still exceeds 80%. So unless velocity distribution of the low temperature, non-observed clouds over the groups 1 to 3 is totally different, the effect is real.

The difference in average velocity between groups 1, 2, and 3 probably reflects properties of the molecular cloud ensemble. Since $\langle V_{mol} - V_H \rangle \simeq 0$, the broad HI peak is probably caused by the superposition of different HI clouds with the same velocity distribution as the molecular clouds. The most important parameters in which the clouds of groups 1 and 3 can be different are the mass and the mean density. The present data are very crude and

Table 5. OH cloud properties in the interval $l = 100°$ to $l = 130°$

Group	1	2	3
T_{ex}(CO)	6.4 ± 1.0 K	5.9 ± 1.4	7.2 ± 1.6
ΔV_{eff}(CO)	6.2 ± 1.9	5.4 ± 1.5	7.7 ± 3.9
Size	0°.44 ± 0.09	0°.37 ± 0.15	0°.61 ± 0.22
V_{CO}	−40.2 ± 7.1	−44.9 ± 5.6	−49.0 ± 4.1
$V_H - V_{CO}$	−3.9 ± 3.9	−1.0 ± 3.4	+3.8 ± 1.9
Number of clouds	8	7	9

our deductions speculative. If group 1 clouds are indeed a factor of 1.5 smaller (Table 5, line 3), their volume is a factor of three less than that of group 3 clouds. The OH column densities in group 1 and 3 differ by at least (due to the assumption $\tau_3 = 0$) a factor of 2.5, thus the masses of the group 1 clouds can be around six times smaller and their mean densities half of those of group 3. Note that the differences will be much larger if kinematic properties of the Perseus arm clouds depend on their mass and their density. Clearly those results have to be confirmed by OH observations of the rest of the ^{12}CO clouds and by ^{13}CO observations.

4.3. The structure of the Perseus arm

4.3.1. The distribution in longitude

In Fig. 10 we show longitude profiles along the Perseus arm between $l = 90°$ and 160° in 2°.5 bins for a number of spiral arm tracers.

A. The gamma ray emission was obtained from Fig. 4 in Mayer-Hasselwander et al. (1982), which is an average flux over latitudes $\pm 5°$. This profile probably is seriously affected by foreground emission.

B. The distribution of the HI emission was obtained from the Maryland Greenbank survey (Westerhout and Wendlandt, 1982). We integrated over velocities between -70 and $-20\,\mathrm{km\,s^{-1}}$ (for $l < 148°$) and between -65 and $-15\,\mathrm{km\,s^{-1}}$ (for $l > 148°$) and over latitudes between $b = -1°.8$ (to avoid Cas A) and $+2°.4$. Because this survey is much better sampled, the binsize was decreased. A further decrease to the 0°.1 resolution would not change the picture.

C. The OB stars were taken from the list of OB associations by Humphreys (1978). The lower line shows only the O stars. Some parts of the arm apparently do not contain such stars. However, this may be a selection effect because these areas are relatively little studied. Sim (1968) lists OB stars along the whole longitude range in Fig. 10, but no distance information is available. In areas with high extinction in the arm (with a high surface density of HII regions and molecular clouds) probably an important fraction of the stars has been missed.

D. The distribution of the number of HII regions situated in the Perseus arm is taken from Fich and Blitz (1984).

E. To get uniform data for the distribution of peak CO temperatures in the clouds near the HII regions in D, we took the data by Blitz et al. (1982). The dashed line represents the distribution for all clouds found by Cong (only for l between 105° and 140°). The scale of the latter is a factor of two smaller and the two datasets were obtained with different telescopes.

F. Radio continuum emission. Because at higher frequencies radio data are less complete, we show the distribution of the 21 cm flux density of the HII regions in D, obtained from Felli and Churchwell (1972), Felli and Harten (1981), Israel (1976) and Kallas and Reich (1980). Because the flux density is distance-dependent, and since the average distance of Perseus arm HII region changes from about 8 kpc at $l = 90°$ to about 3 kpc at $l = 160°$ (see Fich and Blitz, 1984), the peaks near $l = 110°$ and $l = 135°$ would have about the same strength if corrected for this effect.

Comparing the different profiles, most striking are the peaks at $l = 110°$ and $l = 135°$. These are regions of enhanced star and

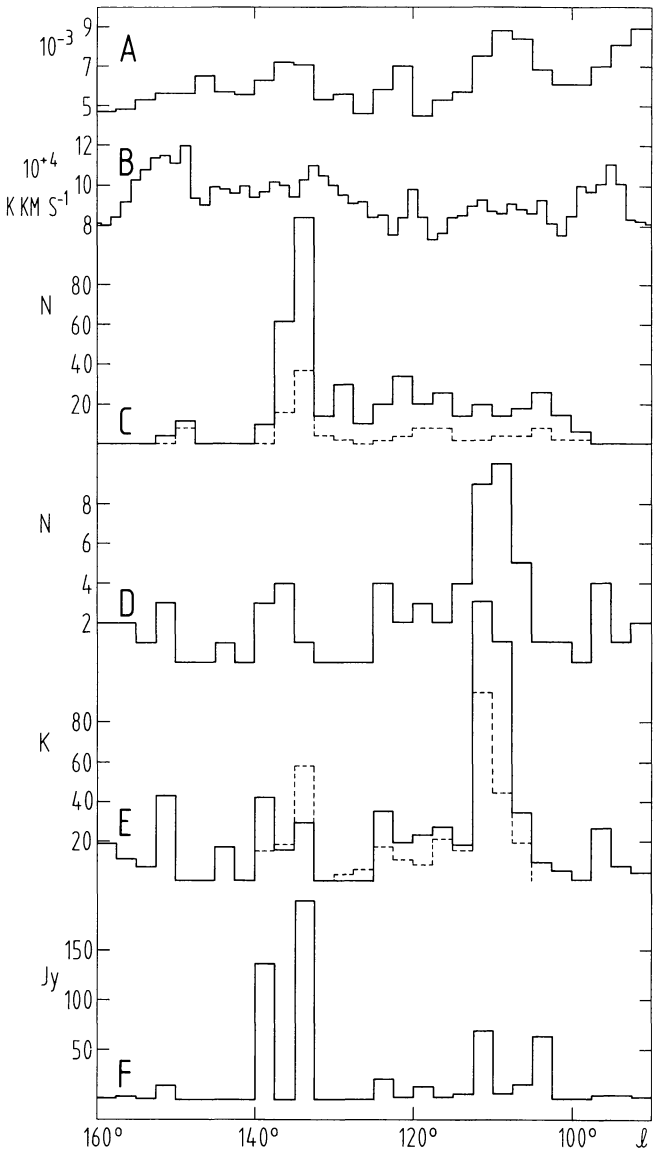

Fig. 10. Profile along Perseus arm of γ-ray emission (A), HI emission (B), OB stars (C), HII regions (D), CO emission (E), HII region 21 cm flux-densities (F)

cloud formation and will be called "concentrations" in the following discussion. The separation between these two concentrations is 1.5–2.0 kpc. The existence of more of such concentrations further down or up the Perseus arm is not known. Around $l = 155°$, Figure 10 shows another group of relatively faint HII regions. Some HII regions at 8 or 9 kpc distance from the sun are present at $l = 70°$ in the region of W58 (Israel, 1976) which probably is another area of activity in the arm. Similar concentrations are observed in other galaxies at typically the same relative distance from each other, for example in the ring in M31 (e.g. Habing et al., 1984). The properties of HII regions along the arm can be analyzed by dividing the area into two parts: $103° < l < 114°$ and $114° < l < 130°$ that both contain 16 HII regions in Sharpless' catalogue. In the first part Kallas and Reich (1980) detected 15 HII regions at 21 cm compared to 10 in the second part. Also the total fluxdensity is higher there (see Fig.

10F). A second result is that in the first part of the arm six HII regions are larger than 30 arcmin, compared to only two in the second part (although this part is closer). From the catalogue by Sharpless (1959) one can find that the HII regions between $l = 108°$ and 114° preferentially are listed in the categories "brightest" and "filamentary", whereas in the other part more regions are listed as "faintest" and "amorphous". One can obtain an indication of the relative ages of the associations by comparing the distribution over spectral types, as published by Humphreys. As far as the division into O and B stars is concerned, this does not result in appreciable differences, except for Cas OB6, which contains twice as many O stars as B stars. Many B stars probably have not been recognized. A more significant result seems to be that the three stars of earliest spectral type are on the average of later type (O9 to B2) for associations in between the concentrations (Cas OB4, Cas OB7, Cas OB2, Cas OB8 and Cep OB5) than for those in or near the concentrations (O5 to O8). This indicates that the concentrations may be the younger parts of the arm. The fact that OH and H_2O masers are only found in the concentrations is supporting this.

In addition to the contrast between a concentration and an intermediate part of the arm, there is also a difference in properties of the HII regions and clouds between the two concentrations. The one near $l = 110°$ contains more HII regions which are much smaller than the concentration at $l = 135°$. The total amount of continuum radiation at 21 cm is smaller as well as the number of OB stars, but both are probably affected by distance or extinction, as mentioned before. The molecular emission is much stronger at $l = 110°$, see also Thaddeus and Dame (1984). Both concentrations are almost invisible in HI, which however may be affected by temperature and density differences. The concentration at $l = 110°$ is stronger in γ-ray emission than the one at $l = 135°$. One can conclude from these facts that the concentration at $l = 135°$ is probably older: the remaining gas content is smaller and a larger fraction of the mass is in stars. The concentration at $l = 110°$ is present at about the whole range of velocities (about -60 to $-35\,\mathrm{km\,s^{-1}}$, see Thaddeus and Dame, 1984) measured also outside the concentrations in that part of the Perseus arm. Combined with the result of the previous section that more massive clouds have a more negative radial velocity, this can be explained in two ways.

1. If one assumes that the clouds in the concentrations are too young to have undergone radial velocity changes (e.g. as in the models by Roberts (1972) or Bash and Peters (1976)). this would mean that the more massive clouds are formed at a more negative radial velocity, must have been formed first to avoid cloud collisions, and presently have a larger distance than the lower mass clouds.

2. However if the radial velocity differences are interpreted as age-effects, which are about $2\,\mathrm{km\,s^{-1}}/10^6\,\mathrm{yr}$ (Bash, priv. comm.), then lower velocity clouds are less massive because on the average a larger fraction of their mass has been consumed in star formation. The age difference between low and high mass clouds must be at least 2×10^7 years and the whole concentration or the clouds must have existed during that time in less condensed form or this "proto-concentration/cloud gas" must have been replenished continuously.

In view of all properties of Perseus arm objects listed in the next section, explanation 2 seems to be more likely.

To obtain a complete understanding of the formation and evolution of such concentrations it would be necessary to study a relatively young concentration (e.g. the one at $l = 110°$) in more detail and to compare it with a quiet part of the arm (e.g. the region $l = 120°$ to 130°). Important parameters are the mass distribution in clouds, HII regions and stars at different radial velocities (or relative ages). With the present data this is not yet possible. Then the results can be compared with models such as that of Elmegreen (1982) who added the influence of self gravity to clouds forming in a Parker instability (Parker, 1966).

4.3.2. Comparison of observations with existing models

Several models have been suggested to explain the structure of this part of the Perseus arm. However, none of them incorporated the properties of the molecular clouds, because these were not yet known. To form a basis for a discussion we first list results from the present observations. Secondly we recapitulate important properties of Perseus arm objects obtained previously by others and thirdly, for completeness, some additional properties of less importance.

1a. The mean velocity of HI in a given longitude interval is the same as that of all molecular clouds in that interval.

1b. The larger and more massive clouds (group 3) have a more negative radial velocity than clouds of lower mass (group 1).

1c. HII regions do not occur preferentially near clouds of either group 1 or group 3. Also there are no differences in properties between those HII regions associated with group 1 and those with group 3.

1d. The small number of clouds between -20 and $-40\,\mathrm{km\,s^{-1}}$ indicates that molecular clouds are at least a factor of five less abundant in the interarm region that in the arm (Cohen et al. 1980). However, Liszt and Burton (1981) showed that kinematics can have consequences as important for the observed velocity distribution as the density contrast.

1e. A weak anti-correlation exists between the positions of molecular clouds and the projected early-type star density in a field around $l = 110°$ (see Wramdemark, 1981).

2a. The radial velocities of stars at the near side of the arm are closer or much closer (between $l = 120°$ and 130°) to that of the clouds than are the velocities of the stars on the far side (see Humphreys, 1976). There is an indication that the earliest type stars have a more negative radial velocity (Martin, 1972).

2b. The distribution of extinction with distance varies from one region to the other. Characteristics for three different regions are: a) it is constant, independent of distance, (b) it shows a steady increase with distance, and c) it shows a discontinuity of 0.5 to 1.5 magnitudes at around 2 to 3 kpc distance (Wramdemark, 1976, 1981; Martin, 1972; Neckel and Klare, 1980).

2c. The space density at early type stars and HII regions has a maximum at a distance of 3 kpc with a very sharp decline towards larger distances (Georgelin, 1975; Crampton et al., 1978; Wramdemark, 1976, 1981).

3a. The mean velocity of all Perseus arm HII regions is on the average $4.3\,\mathrm{km\,s^{-1}}$ more negative than that of all molecular clouds in the same longitude interval ($l = 100°$ to 120°). This agrees with the observations by Israel (1979); it supports the "blister model" for HII regions, but it also indicates that kinematic distances using the HII regions are less reliable.

3b. The apparent radial velocity dispersion of molecular clouds, HII regions, associations and clusters is the same (about $7\,\mathrm{km\,s^{-1}}$). Apparent here means: not corrected for possible systematic motions.

3c. Some stars show optical absorption lines with a more negative velocity than that of the stars (Münch, 1957). The mean value of the velocity of these lines is $-51.4 \pm 10.5\,\mathrm{km\,s^{-1}}$. Perhaps these lines occur in two velocity groups.

3d. A secondary maximum of early type stars and HII regions may exist at 5 to 6 kpc distance ($l = 110°$). However, the number of objects is very small. The distances of most of the objects placed in this larger-distance-arm by Felli and Harten (1981) are kinematical and hence very uncertain. Using a rising rotation curve, Fig. 2 in Fich and Blitz (1984), results in a clear segregation between kinematic and photometric distances of Perseus arm HII regions.

3e. Local OB associations sometimes are associated with an expanding gas shell with expansion velocities up to $15\,\mathrm{km\,s^{-1}}$.

The points 1a, 1e, 2b and 2c indicate that there is a region where HI, molecular clouds and early type stars coexist. This region is at a distance of about 2.5 to 3.5 kpc (at $l = 110°$) and probably has a depth of about 1 kpc.

The mean distance between large molecular clouds of the type detected in CO and studied in this paper is 200 pc and perhaps a factor of two smaller in some specific areas discussed in the preceding subsection. The results of the measurements of extinction as a function of distance indicate that outside the clouds the space inside an arm is not very different from the space in the interarm area. If we take 0°.4 as a typical cloud size, the fraction of the volume of space inside the arm and filled with molecular clouds is $1.5\,10^{-3}$. This is a factor of two larger than the mean value for local clouds, $8\,10^{-4}$ (Wouterloot, 1981). In the Perseus arm this number is a lower limit because of the possible presence of smaller clouds, but it may also be an upper limit if the line of sight depth of the arm is larger than 1 kpc. For the area at 5 to 6 kpc from the galactic center, Liszt and Burton (1981) obtained a volume filling factor of $7\,10^{-3}$.

Several models have been suggested to explain the structure of the Perseus arm.

(i) Rickard (1968) explained the distribution of stellar, HI and interstellar absorption line velocities (3c) by a super-supernova explosion that has occurred within the arm. We think this solution is too drastic. Since this super-supernova explosion appears to be quite an ad-hoc explanation and other explanations work rather well, we reject this hypothesis.

(ii) Verschuur (1973) postulates, from measurments at higher latitudes, the existance of another spiral arm, the α-arm, behind the Persus arm. The HI gas at $b = 0°$, usually ascribed to the Perseus arm, would belong to the α-arm, whereas the HI gas around $-40\,\mathrm{km\,s^{-1}}$, detected at $b = +5°$ to $+10°$ then forms the backside of the Perseus arm. The clouds at high negative velocities, detected by Münch (1957) would be at the frontside of the Perseus arm, expelled by one big HII region which is formed by all associations and young clusters in this area. Verschuur's model is not in agreement with the present observations because the velocity distribution of clouds and HI gas is the same (1a) and because some clouds are associated with HII regions.

(iii) Burton and Bania (1974) and Rohlfs (1974) analysed the HI gas and the stars (Burton and Bania) in connection with deviations from the Schmidt rotation curve. The perturbations from this curve, suggested by Rohlfs, indicate the presence of a shock at 2 kpc distance and of an HI maximum at 4 kpc from the sun, which is behind the stellar arm and in contradiction with the observations. Burton and Bania found that a better correlation between stars and gas exists if the rotation curve is steeper than that of Schmidt. This is in contrast with the findings by Blitz (1979) which indicate that the curve is flatter outside the solar circle.

(iv) The present observations in our opinion best with the model by Roberts (1972), who included the effects of a galactic spiral shock upon the Schmidt rotation curve. In this model the clouds are formed at a past shock velocity of -50 to $-55\,\mathrm{km\,s^{-1}}$. When these clouds subsequently move through the spiral arm, their velocities become less negative and stars form between radial velocities of -50 and $-35\,\mathrm{km\,s^{-1}}$. All observation facts, listed before, are in agreement with this model. One of the new supporting facts is that the most massive clouds have the most negative radial velocity. The older clouds with a less negative velocity have a lower mass because part of their mass has gone into newly formed stars. Point 1c) is not in conflict with this model: the star formation process (so the HII region properties) is not dependent on the total mass of the cloud complex. The absorption lines detected by Münch which are on the average at a somewhat more negative velocity than the clouds can be explained by the molecular clouds, by smaller ones of a velocity of around $-60\,\mathrm{km\,s^{-1}}$ in a state of forming larger clouds and by expanding shells around the associations. The presence of HII regions near group 3 clouds indicates that the onset of star formation has to be fairly rapid after the formation of these clouds because the velocity changes are of the order of 1 to $2\,\mathrm{km\,s^{-1}}$ per 10^6 year. To refine this model it is necessary to derive more accurately the distribution of cloud mass with radial velocity and distance (by means of the related stars) and to use a more realistic rotation curve. Of further interest is the number density of interarm clouds and their properties. They should be observable at low radial velocities but confusion arises with local arm clouds. One has to study age and extent of the associations better. The properties of stars with high and low radial velocities have to be analyzed as well as the direction of the magnetic field at about 3 kpc distance in different parts of the arm.

5. Conclusions

We have made a survey of Perseus arm molecular clouds. Five large clouds were detected in Dwingeloo and mapped in Effelsberg. They have masses of the order of a few times $10^4\,M_\odot$. The clouds show little internal velocity structure. The cloud near W3 shows strong thermal emission at one position. The spectrum of the 1720 MHz OH maser near NGC 7538 shows much structure. We observed a part of the CO clouds in this arm in OH. A new type I OH maser was detected near S152. There appears to be a correlation between properties of the OH clouds and their radial velocity: clouds with a larger OH column density (and probably a larger mass) have a more negative radial velocity. A tentative explanation is presented in terms of the model of the arm by Roberts. The mean number density of this kind of clouds is probably larger in the Perseus arm than in the Local arm, but less than in the "molecular ring" at 5 kpc from the galactic center. The arm contains concentrations of HII regions and molecular clouds, which differ in cloud density, but not in kinematics from the rest of the arm. However, the objects within these concentrations appear to be younger than those in the area in between them.

Acknowledgements. We thank the staff of the Dwingeloo radio observatory, in particular J. Tenkink, and Dr. A. Winnberg at Effelsberg for assistance during the observations. We thank Dr. H.I. Cong for making available his results before publication. This work was supported by a research fellowship from the Organization for the Advancement of Pure Research (ZWO). The Dwingeloo telescope is operated by the Netherlands Foundation for Radio Astronomy.

References

Bash, F.N., Peters, W.L.: 1976, *Astrophys. J.* **205**, 786
Blaauw, A.: 1964, *Annual Review Astron. Astrophys.* **2**, 213
Blitz, L.: 1978, thesis, Columbia University
Blitz, L.: 1979, *Astrophys. J.* **231**, L 115
Blitz, L., Fich, M., Stark, A.A.: 1982, *Astrophys. J. Suppl.* **49**, 183
Burton, W.B., Bania, T.M.: 1974, Astron. Astrophys. **33**, 425
Cohen, R.J., Matthews, N., Few, R.W., Booth, R.S.: 1983, *Monthly Notices Roy. Astron. Soc.* **203**, 1123
Cohen, R.S., Cong, H., Dame, T.M., Thaddeus, P.: 1980, *Astrophys. J.* **239**, L 53
Crampton, D., Georgelin, Y.M., Georgelin, Y.P.: 1978, *Astron. Astrophys.* **66**, 1
Elmegreen, B.G.: 1982, *Astrophys. J.* **253**, 655
Fich, M., Blitz, L.: 1984, *Astrophys. J.* **279**, 125
Felli, M., Churchwell, E.: 1972, *Astron. Astrophys. Suppl.* **5**, 369
Felli, M., Harten, R.H.: 1981, *Astron. Astrophys.* **100**, 28
Georgelin, Y.M.: 1975, thesis, Université de Provence
Goudis, C.: 1979, *Astrophys. Space Sci.* **61**, 417
Guilloteau, S., Lucas, R.: 1981, *Astron. Astrophys.* **101**, L19
Habing, H.J., Miley, G., Young, E., Baud, B., Boggess, N., Clegg, P.E., de Jong, T., Harris, S., Raimond, E., Rowan-Robinson, M., Soifer, B.T.: 1984, *Astrophys. J.* **278**, L59
Hasegawa, T., Sato, F., Fukui, Y.: 1980, Interstellar Molecules, ed. B.H. Andrew, p. 159
Hardebeck, E.G.: 1971 *Astrophys. J.* **170**, 281
Heydari-Malayeri, M., Testor, G., Lortet, M.C.: 1980 *Astron. Astrophys.* **84**, 154
Höglund, B., Gordon, M.A.: 1973, *Astrophys. J.* **182**, 45
Höglund, B., Andersson, C.: 1974, *Astron. Astrophys.* **33**, 389
Hughes, V.A., Harten, R., Van den Bergh, S.: 1981, *Astrophys. J.* **246**, L 127
Humphreys, R.M.: 1976, *Astrophys, J.* **206**, 114
Humphreys, R.M.: 1978, *Astrophys. J. Suppl.* **38**, 309
Israel, F.P.: 1976, thesis, University of Leiden
Israel, F.P.: 1977, *Astron. Astrophys.* **61**, 377
Israel, F.P.: 1978, *Astron. Astrophys.* **70**, 769
Kallas, E., Reich, W.: 1980, *Astron. Astrophys. Suppl.* **42**, 277
Lada, C.J., Elmegreen, B.G., Cong, H.I., Thaddeus, P.: 1978, *Astrophys. J.* **226**, L 39
Liszt, H.S., Burton, W.B.: 1981, *Astrophys. J.* **243**, 778
Martin, N.: 1972, *Astron. Astrophys.* **17**, 253
Mathewson, D.S., Ford, V.L.: 1970, *Mem. Roy. Astron. Soc.* **74**, 139
Mayer-Hasselwander, H.A., Bennet, K., Bignami, C.F., Burcceri, R., Caraveo, P.A., Hermsen, W., Kanbach, C., Leburn, F., Lichti, G.G., Masnou, J.L., Paul, J.A., Pinkau, K., Sacco. B., Scarsi, L., Swanenburg, B.N., Wills, R.D.: 1982, *Astron. Astrophys.* **105**, 164
Milne, D.K.: 1979, *Australian. J. Phys.* **32**, 83
Minn, Y.K., Greenberg, J.M.: 1975, *Astrophys. J.* **196**, 161
Münch, G., 1957: *Astrophys. J.* **125**, 42
Neckel, Th., Klare, G.: 1980, *Astron. Astrophys.* **42**, 251
Parker, E.N.: 1966, *Astrophys. J.* **145**, 811
Read, P.L.: 1980, *Monthly Notices Roy. Astron. Soc.* **192**, 11
Rickard, J.J.: 1968, *Astron. J.* **152**, 1019
Rickard, J.J.: 1979, in The larger scale characteristics of the Galaxy, ed. W.B. Burton, p. 413
Rohlfs, K.: 1974, *Astron. Astrophys.* **35**, 177
Rohlfs, K., Braunsfurth, E., Hills, D.L.: 1977, *Astron. Astrophys. Suppl.* **30**, 369
Roberts, W.W.: 1972, *Astrophys. J.* **173**, 259
Sharpless, S.: 1959, *Astrophys. J. Suppl.* **4**, 257
Sim, M.E.: 1968, *Publ. Royal Obs. Edinburgh* **6**, No. 5
Stark, A.A.: 1980, thesis, Princeton University
Thaddeus, P., Dame, T.M.: 1984, *Occas. Rep. Roy. Obs. Edinburgh*, **13**, 15
Verschuur, G.L.: 1973, *Astron. Astrophys.* **24**, 193
Wendker, H.J., Altenhoff, W.J.: 1977, *Astron. Astrophys.* **54**, 301
Westerhout, G., Wendlandt, H.-U.: 1982, *Astron. Astrophys. Suppl.* **49**, 143
Wouterloot, J.G.A.: 1981, thesis, University of Leiden
Wouterloot, J.G.A.: 1984, *Astron. Astrophys.* **134**, 244
Wramdemark, S.: 1976, *Astron. Astrophys. Suppl.* **26**, 31
Wramdemark, S.: 1981, *Astron. Astrophys. Suppl.* **43**, 103
Wynn-Williams, C.G., Werner M.W., Wilson, W.J.: 1974, *Astrophys. J.* **187**, 41